KJO
pISSN: 1011-8942 eISSN: 2092-9382

Korean J Ophthalmol 2025;39(2):103-113
https://doi.org/10.3341/kjo.2024.0106

Original Article

Anterior Segment Swept-Source Optical Coherence Tomography–based Assessment of Corneal Refractive Profiles in Stevens-Johnson Syndrome/Toxic Epidermal Necrolysis Patients: A Controlled Comparative Study

Dong Hee Ha[1], Seung Hyeun Lee[2], Kyoung Woo Kim[1]

[1]*Department of Ophthalmology, Chung-Ang University Hospital, Chung-Ang University College of Medicine, Seoul, Korea*
[2]*Department of Ophthalmology, Chung-Ang University Gwangmyeong Hospital, Chung-Ang University College of Medicine, Gwangmyeong, Korea*

Purpose: To analyze anterior, posterior, and total corneal refractive profiles and thickness using anterior segment (AS) swept-source optical coherence tomography (SS-OCT) in Stevens-Johnson syndrome (SJS) or toxic epidermal necrolysis (TEN) patients.

Methods: This retrospective study compared 23 eyes from 14 patients with SJS/TEN with 23 eyes from 14 age- and sex-matched controls. AS SS-OCT measured corneal refractive profiles and pachymetry. Parameters included anterior, posterior, and total corneal power values, posterior to anterior curvature ratio, maximal corneal power, and thickness profiles. The SJS/TEN group was subdivided based on corneal opacity presence (subgroup A) or absence (subgroup B).

Results: The SJS/TEN group showed significantly higher corneal astigmatism and maximal corneal power values for both anterior and posterior curvatures. Steep total corneal power and total corneal astigmatism were higher in the SJS/TEN group. The thinnest corneal thickness was lower, and its distance from the corneal vertex was greater in the SJS/TEN group. Subgroup analysis revealed that these differences were primarily attributed to the presence of corneal opacity. Additionally, automated keratometry of the anterior corneal surface showed significantly higher values, including steep, flat, and average keratometry and corneal astigmatism, in the SJS/TEN group.

Conclusions: AS SS-OCT shows significant alterations in both anterior and posterior corneal curvatures in patients with SJS/TEN. These findings emphasize the importance of considering posterior corneal curvature changes in pre-cataract surgery assessments and contact lens prescriptions for patients with SJS/TEN.

Key Words: Anterior segment swept-source optical coherence tomography, Posterior corneal curvature, Stevens-Johnson syndrome, Toxic epidermal necrolysis

Received: August 19, 2024 *Final revision:* December 6, 2024
Accepted: January 20, 2025

Corresponding Author: Kyoung Woo Kim, MD, PhD. Department of Ophthalmology, Chung-Ang University Hospital, Chung-Ang University College of Medicine, 102 Heukseok-ro, Dongjak-gu, Seoul 06973, Korea. Tel: 82-2-6299-1689, Fax: 82-2-825-1666, Email: kkanssa@cau.ac.kr

Stevens-Johnson syndrome (SJS) and toxic epidermal necrolysis (TEN), a more severe SJS variant, are acute inflammatory disorders that can affect multiple systems, including the skin and mucous membranes. They are one of the most severe ocular surface diseases, causing significant

© 2025 The Korean Ophthalmological Society
This is an Open Access journal distributed under the terms of the Creative Commons Attribution Non-Commercial License (http://creativecommons.org/licenses/by-nc/4.0/) which permits unrestricted non-commercial use, distribution, and reproduction in any medium, provided the original work is properly cited.

corneal damage and a substantial threat to vision. During the acute phase, approximately 50% of patients with SJS/TEN experience severe ocular complications including pseudomembranous conjunctivitis and corneal epithelial defects [1]. Early ocular manifestations of the diseases can be diverse, ranging from conjunctival hyperemia to nearly complete sloughing of the entire ocular surface and eyelid margin epithelium [2]. The end-stage status of SJS/TEN is often partial conjunctivalization, progressing toward complete conjunctivalization with accompanying vision loss [3].

Due to the small difference in refractive indexes between posterior cornea (1.367) and the aqueous humor (1.336), the evaluation of posterior cornea curvature has been challenging [4]. However, the recent development of anterior segment optical coherence tomography (AS-OCT) has enabled precise measurements of anterior and posterior corneal parameters in abnormal eyes [5]. With the help of AS-OCT, we can now gain a comprehensive understanding of the alterations in corneal optics caused by SJS/TEN, for both academic evaluation of their progression and appropriate clinical guidance.

Anterior corneal curvature alterations brought on by SJS/TEN have been the main subject of previous research. Due to the usual observances of the signs of SJS/TEN, alterations to the posterior cornea have been largely neglected from research; however, in more severe cases, distortion of the entire cornea, including the posterior surface, may occur. To precisely quantify the total optical changes in the cornea, including modifications in posterior curvature, we have used AS swept-source OCT (SS-OCT). Through this comprehensive analysis, we ultimately intend to deepen our knowledge on ocular involvement of SJS/TEN and contribute to the development of more effective treatment strategies.

Materials and Methods

Ethics statement

This study was approved by the Institutional Review Board of Chung-Ang University Hospital (No. 2408-006-19534). The requirement for informed consent was waived due to the retrospective nature of the study. The entire research process was conducted in accordance with the principles of the Declaration of Helsinki.

Subjects

This study was a retrospective, single center, controlled comparative analysis. This study included 23 eyes from 14 patients with SJS/TEN, assessed using AS SS-OCT between August 2021 and July 2024. The control group, which also included 23 eyes from 14 subjects in a pre-cataract surgery cohort, was matched for age and sex. The SJS/TEN group was further divided into two subgroups depending on the corneal opacity presence: with (subgroup A) and without (subgroup B).

Study design

First, we selected the SJS/TEN group and the control group according to the inclusion criteria. Using AS SS-OCT, we retrospectively evaluated corneal refractive values, including anterior, posterior, and total corneal curvature, as well as corneal pachymetry values in patients with SJS/TEN and controls. Statistical comparisons of these values were conducted between the SJS/TEN group and the control group, as well as among the control group, subgroup A, and subgroup B.

Measurement of corneal refractive and thickness profiles based on AS SS-OCT

Both the SJS/TEN group and the control group underwent measurements using AS SS-OCT (Anterion). On the anterior axial curvature map, the following parameters were obtained: simulated keratometry (Sim K) average (diopters, D), Sim K steep (D), Sim K flat (D), anterior corneal astigmatism (D) at the 3-mm ring, best-fit sphere (BFS; D), maximal keratometry (K_{max}; D), and K_{max} distance (mm) from the corneal vertex within the 8-mm zone. On the posterior axial curvature map, the parameters obtained included K average (D), steep K (D), flat K (D), posterior corneal astigmatism (D), posterior to anterior curvature ratio (P/A ratio) at the 3-mm ring, BFS (D), K_{max} (D), K_{max} distance (mm), and P/A ratio within the 8-mm zone. On the total corneal power map, total corneal power (TCP) profiles were assessed, including TCP average (D), TCP steep (D), TCP flat (D), and total corneal astigmatism (D) at the 3-mm ring. On the corneal pachymetry map, central cor-

neal thickness (μm) and the thinnest point thickness (μm) were measured, and the thinnest point distance (mm) from the corneal vertex was estimated based on the thinnest point x/y (mm) values as part of the corneal thickness profile.

Automated keratometry

Anterior flat K, steep K, average K (K_{ave}), and corneal astigmatism (K_{astig}) values were obtained using automated keratometry (Topcon) in both groups.

Statistical analysis

Statistical analyses were performed using Prism ver. (GraphPad). The D'Agostino-Pearson test was used to evaluate whether the data followed a normal distribution. To compare data between group 1 and group 2, the chi-square test, Fisher exact test, Student *t*-test, or the nonparametric Mann-Whitney *U*-test were applied as appropriate. For comparisons among three groups, one-way analysis of variance followed by Bonferroni *post hoc* test was performed. Values are presented as mean ± standard deviation, with statistical significance set at a *p*-value of <0.05. Anterior and total corneal refractive values, as well as corneal pachymetry values for six eyes that had previously undergone refractive surgery, were excluded from the statistical analyses.

Table 1. Demographic characteristics of the control group and the SJS/TEN group

Characteristic	Control group	SJS/TEN group	*p*-value
No. of patients	14	14	-
No. of eyes	23	23	-
No. of patients with post-refractive surgery	0	3	-
No. of eyes	0	6	-
Age (yr)	50.9 ± 13.3	50.1 ± 11.8	0.858*
Sex			>0.999†
Male	8 (57.1)	7 (50.0)	
Female	6 (42.9)	7 (50.0)	

Values are presented as number only, mean ± standard deviation, or number (%).
SJS = Stevens-Johnson syndrome; TEN = toxic epidermal necrolysis.
*Student *t*-test; †Fisher exact test.

Table 2. Differences in anterior segment swept-source optical coherence tomography–based anterior corneal refractive profiles between the control group and the SJS/TEN group

Variable	Control group	SJS/TEN group	*p*-value
At the anterior 3-mm ring			
Sim K average (D)	42.71 ± 1.52	44.76 ± 7.32	0.231*
Sim K steep (D)	43.20 ±1.52	47.42 ± 8.34	0.052*
Sim K flat (D)	42.24 ± 1.57	42.54 ± 6.91	0.836†
Anterior corneal astigmatism (D)	0.96 ± 0.63	4.88 ± 4.33	<0.001†‡
In the anterior 8-mm zone			
Best-fit sphere (D)	42.40 ±1.38	42.78 ± 6.82	0.626*
K_{max} (D)	43.82 ± 1.35	52.36 ± 10.94	<0.001*‡
K_{max} distance (mm)	1.98 ± 0.82	1.42 ± 1.09	0.018*‡

Values are presented as mean ± standard deviation.
SJS = Stevens-Johnson syndrome; TEN = toxic epidermal necrolysis; Sim K = simulated keratometry; D = diopters; K_{max} = maximal keratometry.
*Mann-Whitney *U*-test; †Student *t*-test; ‡Statistically significant.

Results

Demographics

This study included 23 eyes from 14 patients with SJS/TEN, as well as an equal number of eyes and patients from the control group in a pre-cataract cohort. Table 1 presents the demographic information of both groups. The control group comprised six women (42.9%) and eight men (57.1%), with an average age of 50.9 ± 13.3 years. The SJS/TEN group consisted of seven women (50.0%) and seven men (50.0%), with an average age of 50.1 ± 11.8 years. The age and sex distributions between the two groups did not differ significantly ($p = 0.858$ and $p > 0.999$, respectively).

Differences in AS SS-OCT–based anterior corneal refractive profiles between the control group and the SJS/TEN group

In the control group, the anterior astigmatism at the 3-mm ring, K_{max} within the 8-mm zone, and K_{max} distance within the 8-mm zone were measured at 0.96 ± 0.63 D, 43.82 ± 1.35 D, and 1.98 ± 0.82 mm, respectively. These measurements showed significant differences compared to those in the SJS/TEN group, where the corresponding values were 4.88 ± 4.33 D, 52.36 ± 10.94 D, and 1.42 ± 1.09 mm ($p < 0.001$, $p < 0.001$, and $p = 0.018$, respectively). However, no significant differences were observed between the two groups in terms of Sim K average, Sim K steep, Sim K flat, and BFS in the anterior corneal refractive profiles (Table 2).

Table 3. Differences in anterior segment swept-source optical coherence tomography–based posterior corneal refractive profiles between the control group and the SJS/TEN group

Variable	Control group	SJS/TEN group	*p*-value
At the posterior 3-mm ring			
K average (D)	–6.13 ± 0.26	–6.08 ± 0.62	0.776*
Steep K (D)	–6.30 ± 0.29	–6.41 ± 0.50	0.391†
Flat K (D)	–5.96 ± 0.25	–5.81 ± 0.73	0.903*
Posterior corneal astigmatism (D)	–0.34 ± 0.11	–0.60 ± 0.47	0.036*‡
P/A ratio	0.83 ± 0.03	0.86 ± 0.20	0.320*
In the posterior 8-mm zone			
Best-fit sphere (D)	–6.01 ± 0.21	–6.01 ± 0.45	0.938†
K_{max} (D)	–6.39 ± 0.30	–6.92 ± 0.98	0.003*‡
K_{max} distance (mm)	1.60 ± 0.91	1.74 ± 0.94	0.614†
P/A ratio	0.83 ± 0.02	0.83 ± 0.02	0.436*

Values are presented as mean ± standard deviation.
SJS = Stevens-Johnson syndrome; TEN = toxic epidermal necrolysis; K = keratometry; D = diopters; P/A ratio = posterior to anterior curvature ratio; K_{max} = maximal keratometry.
*Mann-Whitney *U*-test; †Student *t*-test; ‡Statistically significant.

Table 4. Differences in anterior segment swept-source optical coherence tomography–based total corneal refractive profiles between the control group and the SJS/TEN group

At the TCP 3-mm ring	Control group	SJS/TEN group	*p*-value
TCP average (D)	42.09 ± 1.56	44.52 ± 5.53	0.053*
TCP steep (D)	42.52 ± 1.57	47.06 ± 7.18	0.006†‡
TCP flat (D)	41.75 ± 1.55	41.98 ± 4.77	0.830*
Total corneal astigmatism (D)	0.85 ± 0.63	5.08 ± 5.10	<0.001*‡

Values are presented as mean ± standard deviation.
SJS = Stevens-Johnson syndrome; TEN = toxic epidermal necrolysis; TCP = total corneal power; D = diopters.
*Student *t*-test; †Mann-Whitney *U*-test; ‡Statistically significant.

Differences in AS SS-OCT–based posterior corneal refractive profiles between the control group and the SJS/TEN group

The differences in posterior corneal refractive profiles between the two groups are shown in Table 3. In the control group, the values of posterior astigmatism at the 3-mm ring and K_{max} within the 8-mm zone were –0.34 ± 0.11 D and –6.39 ± 0.30 D, respectively. In comparison, the corresponding measurements in the SJS/TEN group were –0.60 ± 0.47 D and –6.92 ± 0.98 D, respectively, showing significant differences (p = 0.036 and p = 0.003, respectively). However, no significant differences were observed between the two groups in other posterior corneal refractive profile parameters, including K average, steep K, flat K, P/A ratio, BFS, and K_{max} distance.

Differences in AS SS-OCT–based total corneal refractive profiles between the control group and the SJS/TEN group

Table 4 illustrates the differences in total corneal profiles between the groups. In the control group, the measurements of TCP steep and total corneal astigmatism at the 3-mm ring were 42.52 ± 1.57 D and 0.85 ± 0.63 D, respectively. These values were significantly different from those in the SJS/TEN group, where the corresponding measurements were 47.06 ± 7.18 D and 5.08 ± 5.10 D, respectively (p = 0.006 and p < 0.001, respectively). However, no significant differences were observed between the TCP average and TCP flat values of the two groups.

Differences in corneal thickness profiles between the control group and the SJS/TEN group

In the control group, the thinnest point thickness was measured at 543.80 ± 32.79 μm, and the thinnest point distance was 0.65 ± 0.27 mm. In contrast, in the SJS/TEN group, the thinnest corneal thickness was lower at 477.50 ± 124.10 μm (p = 0.019), and the thinnest point distance was greater at 1.82 ± 1.26 mm (p < 0.001) (Table 5). However, no significant difference was observed in the central corneal thickness between the two groups.

Differences in automated keratometry–based anterior corneal refractive profiles between the control group and the SJS/TEN group

Considering that automated keratometry is more commonly used than AS SS-OCT in routine ophthalmic surgeries, including cataract surgery, an additional comparative analysis of anterior K values obtained through automated keratometry was conducted between the two groups. The values of all parameters including flat K, steep K, K_{ave}, and K_{astig} were significantly higher (p = 0.029, p = 0.003, p = 0.003, and p < 0.001, respectively) in the SJS/TEN group compared to the control group (Table 6).

Table 6. Differences in automated keratometry–based anterior corneal refractive profiles between the corneal group and the SJS/TEN group

Variable	Control group	SJS/TEN group	p-value
Flat K (D)	42.53 ± 1.68	45.12 ± 4.08	0.029*†
Steep K (D)	42.83 ± 1.49	46.65 ± 5.46	0.003†‡
K_{ave} (D)	42.74 ± 1.53	45.73 ± 4.16	0.003†‡
K_{astig} (D)	–0.73 ± 0.55	–2.87 ± 2.59	<0.001*†

Values are presented as mean ± standard deviation.
SJS = Stevens-Johnson syndrome; TEN = toxic epidermal necrolysis; K = keratometry; D = diopters; K_{ave} = average keratometry; K_{astig} = corneal astigmatism.
*Mann-Whitney U-test; †Statistically significant; ‡Student t-test.

Table 5. Differences in anterior segment swept-source optical coherence tomography–based corneal thickness profiles between the corneal group and the SJS/TEN group

Variable	Control group	SJS/TEN group	p-value*
Central corneal thickness (vertex) (μm)	547.20 ± 32.85	538.90 ± 118.90	0.750
Thinnest point thickness (μm)	543.80 ± 32.79	477.50 ± 124.10	0.019†
Thinnest point distance (mm)	0.65 ± 0.27	1.82 ± 1.26	<0.001†

Values are presented as mean ± standard deviation.
SJS = Stevens-Johnson syndrome; TEN = toxic epidermal necrolysis.
*Student t-test; †Statistically significant.

Table 7. Differences in anterior segment swept-source optical coherence tomography–based anterior, posterior, and total corneal refractive profiles, and corneal thickness profiles among the control group and the SJS/TEN subgroups, categorized by the presence of corneal opacity

Variable	Control group	SJS/TEN group		*p*-value			
		Subgroup A (with corneal opacity)	Subgroup B (without corneal opacity)	ANOVA	*post hoc* between groups		
					Control vs. A	Control vs. B	A vs. B
No. of eyes	23	12	11	-	-	-	-
At the anterior 3-mm ring							
Sim K average (D)	42.71 ± 1.52	45.58 ± 9.28	43.39 ± 1.60	0.302		-	-
Sim K steep (D)	43.20 ± 1.52	49.50 ± 10.07	43.96 ± 1.75	<0.001*	0.009*	>0.999	0.140
Sim K flat (D)	42.24 ± 1.57	42.37 ± 8.83	42.84 ± 1.57	0.960			
Anterior corneal astigmatism (D)	0.96 ± 0.63	7.14 ± 3.94	1.12 ± 0.93	<0.001*	<0.001*	>0.999	<0.001*
At the anterior 8-mm zone							
BFS (D)	42.40 ± 1.38	42.95 ± 8.59	42.46 ± 1.14	0.948	-	-	-
K_{max} (D)	43.82 ± 1.35	56.46 ± 11.58	44.85 ± 3.19	<0.001*	<0.001*	>0.999	0.002*
K_{max} distance (mm)	1.98 ± 0.82	1.44 ± 1.28	1.40 ± 0.71	0.208	-	-	-
At the posterior 3-mm ring							
K average (D)	–6.13 ± 0.26	–5.91 ± 0.86	–6.24 ± 0.20	0.258	-	-	-
Steep K (D)	–6.30 ± 0.29	–6.33 ± 0.68	–6.48 ± 0.26	0.501	-	-	-
Flat K (D)	–5.96 ± 0.25	–5.58 ± 1.01	–6.02 ± 0.19	0.109	-	-	-
Posterior corneal astigmatism (D)	–0.34 ± 0.11	–0.75 ± 0.63	–0.45 ± 0.18	0.006*	0.005*	>0.999	0.118
P/A ratio	0.83 ± 0.03	0.89 ± 0.25	0.82 ± 0.02	0.396	-	-	-
At the posterior 8-mm zone							
BFS (D)	–6.01 ± 0.21	–5.88 ± 0.61	–6.12 ± 0.19	0.261	-	-	-
K_{max} (D)	–6.39 ± 0.30	–7.25 ± 1.30	–6.59 ± 0.29	0.006*	0.004*	>0.999	0.090
K_{max} distance (mm)	1.60 ± 0.91	2.06 ± 1.14	1.40 ± 0.55	0.211	-	-	-
P/A ratio	0.83 ± 0.02	0.85 ± 0.02	0.81 ± 0.01	0.005*	0.133	0.061	0.004*
At the TCP 3-mm ring							
TCP average (D)	42.09 ± 1.56	45.69 ± 6.91	42.76 ± 1.76	0.050*	0.046*	>0.999	0.392
TCP steep (D)	42.52 ± 1.57	49.55 ± 8.39	43.31 ± 1.94	<0.001*	<0.001*	>0.999	0.026*
TCP flat (D)	41.75 ± 1.55	41.82 ± 6.16	42.21 ± 1.65	0.953	-	-	-
Total corneal astigmatism (D)	0.85 ± 0.63	7.73 ± 5.03	1.10 ± 0.79	<0.001*	<0.001*	>0.999	<0.001*
Corneal thickness							
Central corneal thickness (vertex) (μm)	547.20 ± 32.85	541.6 ± 150.5	534.3 ± 39.68	0.937	-	-	-
Thinnest point thickness (μm)	543.80 ± 32.79	447.0 ± 148.2	528.3 ± 41.58	0.010*	0.009*	>0.999	0.169
Thinnest point distance (mm)	0.65 ± 0.27	2.34 ± 1.32	0.94 ± 0.35	<0.001*	<0.001*	>0.999	0.001*

Values are presented as mean ± standard deviation.
SJS = Stevens-Johnson syndrome; TEN = toxic epidermal necrolysis; ANOVA = analysis of variance; Sim K = simulated keratometry; D = diopters; BFS = best-fit sphere; K_{max} = maximal keratometry; P/A ratio = posterior to anterior curvature ratio; TCP = total corneal power.
*Statistically significant.

Differences in AS SS-OCT–based anterior, posterior, and total corneal refractive profiles and corneal thickness profiles among the control group and the SJS/TEN group with and without corneal opacity

Next, to verify whether SJS/TEN subjects with corneal opacity (subgroup A) exhibit different AS SS-OCT features compared to those without corneal opacity (subgroup B), we compared the values of subgroup A and subgroup B with those of the control group.

Sim K steep ($p < 0.001$) and anterior corneal astigmatism ($p < 0.001$) at the anterior 3-mm ring, K_{max} within the anterior 8-mm zone ($p < 0.001$), posterior corneal astigmatism at the posterior 3-mm ring ($p = 0.006$), K_{max} ($p = 0.006$) and P/A ratio within the posterior 8-mm zone ($p = 0.005$), and TCP average ($p = 0.050$), TCP steep ($p < 0.001$), and total corneal astigmatism at the TCP 3-mm ring ($p < 0.001$) were highest in subgroup A among three groups (Table 7).

Among these parameters, anterior corneal astigmatism at the anterior 3-mm ring, K_{max} within the anterior 8-mm zone, and TCP steep and total corneal astigmatism at the TCP 3-mm ring were significantly higher in subgroup A compared to both the control group ($p < 0.001$ for all) and subgroup B ($p < 0.001$, $p = 0.002$, $p = 0.026$, and $p < 0.001$, respectively). Sim K steep at the anterior 3-mm ring, posterior corneal astigmatism at the posterior 3-mm ring, K_{max} within the posterior 8-mm zone, and TCP average at the TCP 3-mm ring were higher in subgroup A compared only to the control group ($p = 0.009$, $p = 0.005$, $p = 0.004$, and $p = 0.046$, respectively). On the other hand, the P/A ratio within the posterior 8-mm zone was significantly higher in subgroup A compared only to subgroup B ($p = 0.004$) (Table 7).

Among corneal thickness parameters, central corneal thickness values did not differ significantly among the groups ($p = 0.937$). However, the thinnest point thickness was lowest in subgroup B ($p = 0.010$), with significant differences compared to the control group ($p = 0.009$). The thinnest point distance was longest in subgroup A ($p < 0.001$), with significant differences observed compared to both the control group ($p < 0.001$) and subgroup B ($p = 0.001$) (Table 7).

AS SS-OCT findings in the control group and the SJS/TEN group

Representative AS SS-OCT findings from the anterior axial curvature map, anterior tangential curvature map, posterior axial curvature map, and corneal pachymetry map are presented for the control group (Fig. 1A–1D), the SJS/TEN group without corneal opacity (Fig. 1E–1H), and the SJS/TEN group with corneal opacity (Fig. 1I–1L). In SJS/TEN cases with corneal opacity, pronounced posterior curvature irregularity as well as severe anterior corneal irregular astigmatism is observed (Fig. 1J, 1L).

Discussion

The possibility of a long-term progression of ocular surface cicatrization is well-established from earlier research on SJS/TEN. There are two categories of ocular surface failures: conjunctival failure, which includes squamous metaplasia, symblepharon, and fornix shortening; and limbal stem cell failure, which is characterized by conjunctivalization, corneal neovascularization, and persistent epithelial defects [3]. The corneal damage through limbal stem cell failure or scarring is one of the most devastating ocular outcomes of SJS/TEN.

To accurately diagnose a corneal pathology and assess its structure, the most accurate corneal measurements are needed. Accurate measurements of both the anterior and posterior cornea are essential not only for the diagnosis but also for the treatment of different ocular diseases [6]. This requirement also applies to SJS/TEN, which affects the cornea. Despite this, research examining the quantitative effect of SJS/TEN on corneal optical characteristics has been lacking. Using the AS SS-OCT, we quantitatively assessed anterior, posterior, and total corneal curvature alterations, as well as corneal pachmetry features, in patients with SJS or TEN. The accurate corneal measurements are important because SJS/TEN-induced limbal stem cell deficit can alter corneal structure in a way that negatively impacts visual function and quality of life in general [7].

Since its introduction, AS-OCT has become crucial for assessing the cornea and anterior eye segment. AS-OCT has been discovered to exceed Placido-Scheimpflug imaging in reproducibility for central corneal thickness and keratometry measurements after laser *in situ* keratomileu-

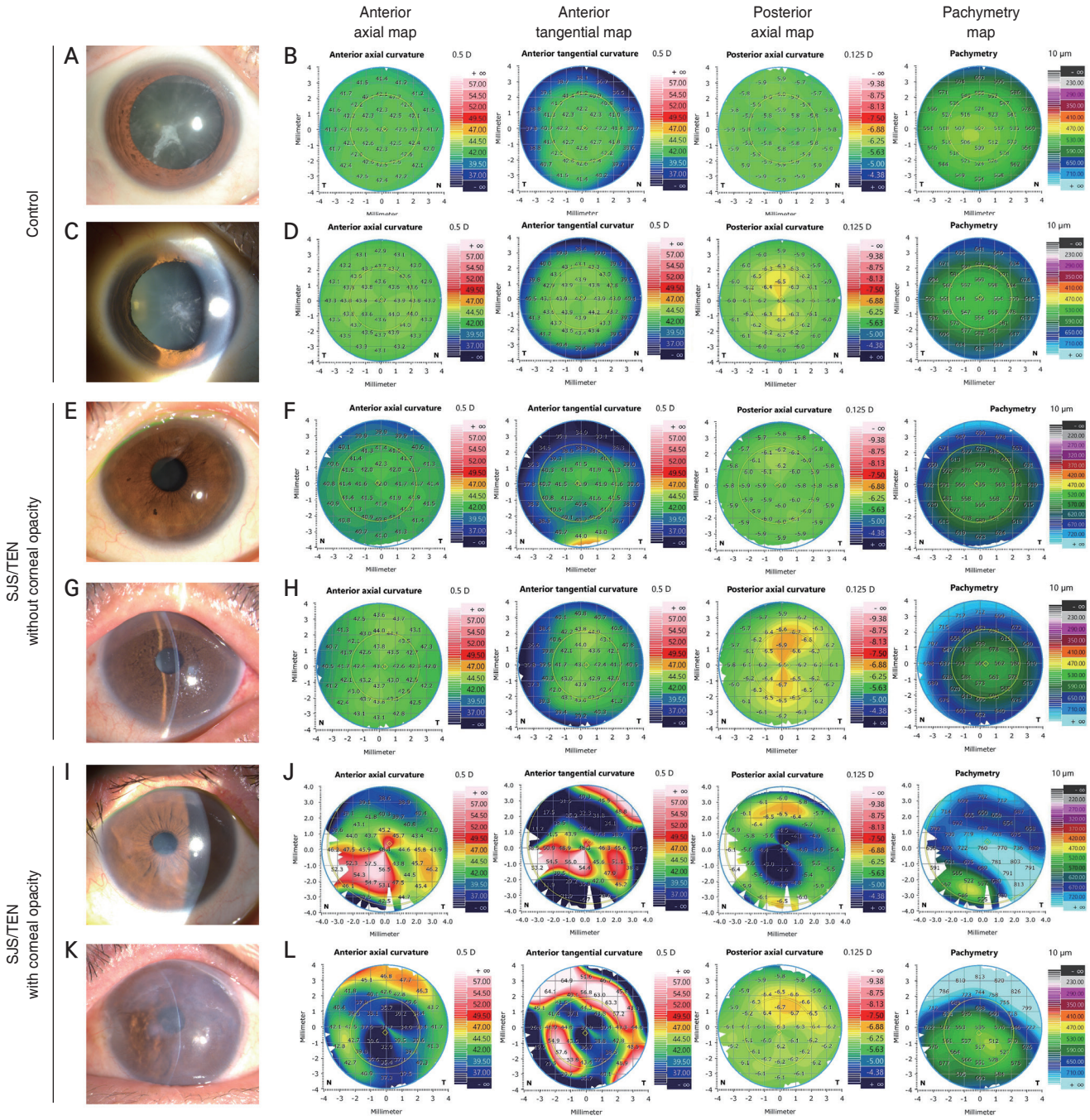

Fig. 1. Representative slit-lamp biomicroscopic photographs and anterior segment swept-source optical coherence tomography corneal findings, including anterior axial maps, anterior tangential maps, posterior axial maps, and corneal pachymetry maps, from the control group and the Stevens-Johnson syndrome (SJS)/toxic epidermal necrolysis (TEN) group. (A–D) Two representative normal case. Regular, mild corneal astigmatism on both the anterior and posterior corneal surfaces is observed in the two normal cases from the control group. (E–H) Two representative SJS/TEN cases without corneal opacity. Regular anterior and posterior corneal astigmatism similar to that in normal cases is noted. (I–L) Two representative SJS/TEN cases with corneal opacity. Irregular and severe corneal astigmatism on both the anterior and posterior corneal surfaces is observed, along with inferior-dominant corneal thinning in both cases.

sis (LASIK) [8]. The high-quality, detailed anterior and posterior cornea maps are essential for diagnosing and managing conditions like corneal ectasia, assessing corneal astigmatism, or planning refractive surgery [6]. Notably, AS SS-OCT, a type of AS-OCT, uses a high-speed, narrow-bandwidth light source to obtain up to 2 million

A-scans per second [9–11]. AS SS-OCT provides detailed maps such as anterior and posterior curvature, elevation, TCP, wavefront, and pachymetry with superior depth range, decreased sensitivity roll-off, and reduced susceptibility to motion artifacts [12]. Due to its excellent performance, AS SS-OCT is increasingly used for precise corneal measurement in many clinical practices: we have used AS SS-OCT to gather accurate measurements of the corneal parameters.

As discussed in the results of this study, corneal astigmatism and K_{max} values were significantly higher in SJS/TEN group for both the anterior and posterior corneal curvatures. There have been prior studies investigating the changes in the anterior surface of patients with SJS/TEN [13]. Many previous studies have also discovered a positive correlation between the anterior and posterior corneal asphericities [14]. However, studies investigating the posterior cornea have been scarce. In this current study, the posterior astigmatisms of both the control group and the SJS/TEN group fall within the known average range of posterior corneal surface (−0.26 to −0.78 D) [15,16], and there is a significant difference between two groups. Although the posterior corneal surface only contributes to about 10% of the total refractive power of the eye, a precise assessment of its morphology is important because evaluations neglecting the posterior corneal surface measurements may cause significant deviations from the precise corneal astigmatism estimation [14]. We think that the possibility of extensive corneal impairment requires an accurate assessment of the posterior cornea in patients with SJS/TEN for better depiction of the damage.

The subgroup analysis comparing SJS/TEN cases with and without corneal opacity provided valuable insights into the severity of corneal involvement in these conditions. Patients with SJS/TEN with corneal opacity (subgroup A) demonstrated significantly higher values for several corneal parameters, including anterior and posterior corneal astigmatism, anterior and posterior K_{max}, and total corneal astigmatism compared to the control group. Notably, patients with SJS/TEN without corneal opacity (subgroup B) did not show significant differences in all of parameters compared to the control group (Table 7). This finding suggests that the presence of corneal opacity may be a crucial indicator of more severe corneal involvement in SJS/TEN. The observation of higher values in anterior corneal astigmatism, K_{max} within the anterior 8-mm zone, TCP steep, and total corneal astigmatism in subgroup A compared to both the control group and subgroup B underscores the impact of corneal opacity on corneal structure and function.

The identification of severe posterior corneal changes may influence the pre-cataract surgery assessments and the effectiveness of treatments designed to correct anterior curvature issues, such as scleral lenses. When conducting a cataract surgery, neglecting the posterior astigmatism can cause some critical errors in correcting the astigmatism. Because most of the eyes have a posterior astigmatism, which is against-the-rule, if this negligence occurs in toric intraocular lens use, it overcorrects with-the-rule astigmatism and undercorrects against-the-rule astigmatism [14]. Similar to the result of a miscalculation in cataract surgery, an inaccurate calculation of the amount of posterior corneal astigmatism with a steep meridian in prescription of scleral lenses may result in the inaccurate corrections of the astigmatism [14]. We consider that the AS SS-OCT can be beneficial for patients with SJS/TEN by objectively detecting the overall optical damages of the cornea that can impact the subsequent treatments.

Another important finding of our current study is that corneal ectasia is noted in the SJS/TEN group. Generally, the corneal ectasia progression shows a consistent change in at least two of the following parameters: (1) progressive steepening of the anterior corneal surface; (2) progressive steepening of the posterior corneal surface; or (3) progressive thinning and/or an increase in the rate of corneal thickness change from the periphery to the thinnest point [17]. From previous research, the prevalence of corneal ectasia among patients with SJS/TEN as compared with that of the general population was also statistically significant [18]. However, there has been a lack of reports on the prevalence of corneal ectasia and SJS/TEN as associated disorders. The results of our study quantitively show corneal ectasia in the SJS/TEN group.

Additional point to note is that the anterior and posterior steep, flat, and average corneal powers, as well as the BFS and P/A ratio values, did not differ significantly between two groups. This may be attributed to the fact that localized changes induced by SJS/TEN may not translate into global corneal curvature changes. SJS/TEN can cause more patchy, peripheral thinning and scarring rather than uniform thinning at the center. For example, severe inflammation and ulceration of the tarsal conjunctiva and

eyelid margins in patients with acute SJS/TEN can cause tarsal scarring, eyelid margin keratinization, and lipid tear deficiency [18]. These adnexal changes can indirectly induce localized scars on cornea via microtraumas. Since this study is retrospective, there are certain limitation in observing the progression and mechanisms of corneal changes. It would be beneficial to investigate these alterations in future studies.

The limitations of this current study are as follows: first, it was a retrospective study, not a prospective study. Due to the rarity of SJS/TEN, it is hard to collect data prospectively from enough patients. Second, the SJS/TEN cases that had undergone ocular refractive surgeries were excluded for the analysis of anterior and total corneal profiles. This exclusion further decreased the number of patients from statistical analysis of those aspects; however, it was inevitable to increase the validity of the results. Moreover, future studies can aim to evaluate the correlations between the ocular surface severity grades and the degrees of corneal axial changes.

In conclusion, AS SS-OCT allows for the objective detection of corneal damage, providing patients with SJS/TEN with valuable long-term monitoring. Since AS SS-OCT shows significant alterations in the posterior corneal curvature, we need to consider posterior corneal curvature changes in pre-cataract surgery evaluations and contact lens prescriptions in patients with SJS/TEN. We also recommend cautious interpretation of these clinically relevant AS SS-OCT parameters when used in treatment decision-making.

Conflicts of Interest: None.
Acknowledgements: None.
Funding: None.

References

1. Ueta M. Pathogenesis of Stevens-Johnson syndrome/toxic epidermal necrolysis with severe ocular complications. *Front Med (Lausanne)* 2021;8:651247.
2. Metcalfe D, Iqbal O, Chodosh J, et al. Acute and chronic management of ocular disease in Stevens Johnson syndrome/toxic epidermal necrolysis in the USA. *Front Med (Lausanne)* 2021;8:662897.
3. Yoshikawa Y, Ueta M, Fukuoka H, et al. Long-term progression of ocular surface disease in Stevens-Johnson syndrome and toxic epidermal necrolysis. *Cornea* 2020;39:745–53.
4. Muzyka-Wozniak M, Oleszko A, Grzybowski A. Measurements of anterior and posterior corneal curvatures with OCT and scheimpflug biometers in patients with low total corneal astigmatism. *J Clin Med* 2022;11:6921.
5. Nakagawa T, Maeda N, Higashiura R, et al. Corneal topographic analysis in patients with keratoconus using 3-dimensional anterior segment optical coherence tomography. *J Cataract Refract Surg* 2011;37:1871–8.
6. Tana-Rivero P, Aguilar-Corcoles S, Ruiz-Mesa R, Montes-Mico R. Repeatability of whole-cornea measurements using a new swept-source optical coherence tomographer. *Eur J Ophthalmol* 2021;31:1709–19.
7. Sheppard JD, Mansur A, Comstock TL, Hovanesian JA. An update on the surgical management of pterygium and the role of loteprednol etabonate ointment. *Clin Ophthalmol* 2014;8:1105–18.
8. Chan TC, Liu D, Yu M, Jhanji V. Longitudinal evaluation of posterior corneal elevation after laser refractive surgery using swept-source optical coherence tomography. *Ophthalmology* 2015;122:687–92.
9. Huo T, Wang C, Zhang X, et al. Ultrahigh-speed optical coherence tomography utilizing all-optical 40 MHz swept-source. *J Biomed Opt* 2015;20:030503.
10. Kolb JP, Klein T, Kufner CL, et al. Ultra-widefield retinal MHz-OCT imaging with up to 100 degrees viewing angle. *Biomed Opt Express* 2015;6:1534–52.
11. Zhi Z, Qin W, Wang J, et al. 4D optical coherence tomography-based micro-angiography achieved by 1.6-MHz FDML swept source. *Opt Lett* 2015;40:1779–82.
12. Gora M, Karnowski K, Szkulmowski M, et al. Ultra high-speed swept source OCT imaging of the anterior segment of human eye at 200 kHz with adjustable imaging range. *Opt Express* 2009;17:14880–94.
13. Ibrahim OM, Yagi-Yaguchi Y, Noma H, et al. Corneal higher-order aberrations in Stevens-Johnson syndrome and toxic epidermal necrolysis. *Ocul Surf* 2019;17:722–8.
14. Mohammadi SF, Khorrami-Nejad M, Hamidirad M. Posterior corneal astigmatism: a review article. *Clin Optom (Auckl)* 2019;11:85–96.
15. Dubbelman M, Sicam VA, Van der Heijde GL. The shape of the anterior and posterior surface of the aging human cornea. *Vision Res* 2006;46:993–1001.
16. Koch DD, Ali SF, Weikert MP, et al. Contribution of poste-

rior corneal astigmatism to total corneal astigmatism. *J Cataract Refract Surg* 2012;38:2080–7.

17. Ambrosio R. Post-LASIK ectasia: twenty years of a conundrum. *Semin Ophthalmol* 2019;34:66–8.
18. Saeed HN, Kohanim S, Le HG, et al. Stevens-Johnson syndrome and corneal ectasia: management and a case for association. *Am J Ophthalmol* 2016;169:276–81.